

Supporting Information

In Vivo EPR Characterization of Semi-Synthetic [FeFe] Hydrogenases

*Livia S. Mészáros, Brigitta Németh, Charlène Esmieu, Pierre Ceccaldi, and Gustav Berggren**

anie_201710740_sm_miscellaneous_information.pdf

Author Contributions

L.M. Data curation: Equal; Formal analysis: Supporting; Investigation: Lead; Writing—review & editing: Equal

B.N. Data curation: Supporting; Investigation: Supporting; Methodology: Supporting; Writing—original draft: Supporting; Writing—review & editing: Supporting

C.E. Conceptualization: Supporting; Data curation: Supporting; Investigation: Supporting; Methodology: Supporting; Writing—original draft: Supporting; Writing—review & editing: Supporting

P.C. Formal analysis: Supporting; Validation: Supporting; Visualization: Supporting; Writing—review & editing: Supporting

G.B. Conceptualization: Lead; Data curation: Equal; Formal analysis: Lead; Funding acquisition: Lead; Investigation: Supporting; Methodology: Equal; Project administration: Lead; Resources: Lead; Supervision: Lead; Writing—original draft: Lead; Writing—review & editing: Lead.

TABLE OF CONTENTS

Figure S-1. SDS-PAGE analysis to determine the expression level of the apo-HydA1 protein	2
Figure S-2. X-band EPR signals observed for BL21(DE3) cells with and without expression of apo – HydA1, and their respective microwave power dependence	3
Figure S-3. EPR spectra recorded on whole cell samples of BL21(DE3) not expressing HydA1 incubated with $[2\text{Fe}]^{\text{pdt}}$	4
Figure S-4. Microwave power dependence of $[2\text{Fe}]^{\text{pdt}}$ -HydA1 in whole cells at 5 K	5
Figure S-5. Microwave power dependence of $[2\text{Fe}]^{\text{pdt}}$ -HydA1 in whole cells at 10 K	6
Figure S-6. Microwave power dependence of $[2\text{Fe}]^{\text{pdt}}$ -HydA1 in whole cells at 20 K	7
Figure S-7. Microwave power dependence of $[2\text{Fe}]^{\text{pdt}}$ -HydA1 _{pur} at 5 K	8
Figure S-8. Microwave power dependence of $[2\text{Fe}]^{\text{pdt}}$ -HydA1 _{pur} at 10 K	9
Figure S-9. Microwave power dependence of $[2\text{Fe}]^{\text{pdt}}$ -HydA1 _{pur} at 20 K	10
Figure S-10. Temperature dependence of $[2\text{Fe}]^{\text{pdt}}$ -HydA1 in whole cells	11
Figure S-11. Temperature dependence of $[2\text{Fe}]^{\text{pdt}}$ -HydA1 _{pur}	12
Figure S-12. Microwave power saturation behavior of $[2\text{Fe}]^{\text{pdt}}$ -HydA1 at 5 K	13
Figure S-13. Microwave power saturation behavior of $[2\text{Fe}]^{\text{pdt}}$ -HydA1 at 10 K	14
Figure S-14. Microwave power saturation behavior of $[2\text{Fe}]^{\text{pdt}}$ -HydA1 at 20 K	15
Figure S-16. Formation of $[2\text{Fe}]^{\text{pdt}}$ -HydA1 under in vivo conditions monitored by EPR spectroscopy	17
Figure S-17. Reduction of $[2\text{Fe}]^{\text{pdt}}$ -HydA1 after cell lysis	18
Figure S-18. Stability of $[2\text{Fe}]^{\text{pdt}}$ -HydA1 in an H_{ox} -like state under in vivo conditions	19
Figure S-19. $[2\text{Fe}]^{\text{pdt}}$ -HydA1 oxidation under in vivo conditions	20
Figure S-20. Reduction of $[2\text{Fe}]^{\text{adt}}$ -HydA1 after cell lysis	21
Figure S-21. Comparison of the microwave power dependence in the H_{ox} -CO signal region	22
Figure S-22. Comparison of the microwave power dependence behavior in the H_{ox} signal region	23
Figure S-23. Simulation of the EPR spectrum of $[2\text{Fe}]^{\text{adt}}$ -HydA1 _{pur} recorded at 10K	24
Figure S-24. Simulation of the EPR spectrum of $[2\text{Fe}]^{\text{adt}}$ -HydA1 in whole cells recorded at 10K	25
Table S-1. Simulation parameters of the $\text{H}_{\text{ox}}-[2\text{Fe}]^{\text{pdt}}$ (= H_{ox} -like), H_{ox} and H_{ox} -CO species	26
Table S-2. Comparison of the g values observed in this work with the previous literature data	27
Experimental Section	28
General	28
Synthesis of $(\text{Et}_4\text{N})_2[\text{Fe}_2(\text{pdt})(\text{CO})_4(\text{CN})_2]$ ($[2\text{Fe}]^{\text{pdt}}$) and $(\text{Et}_4\text{N})_2[\text{Fe}_2(\text{adt})(\text{CO})_4(\text{CN})_2]$ ($[2\text{Fe}]^{\text{adt}}$)	28
Overexpression of the apo-HydA1 hydrogenase	28
In vivo formation of $[2\text{Fe}]^{\text{pdt}}$ - and $[2\text{Fe}]^{\text{adt}}$ -HydA1	28
Whole cell EPR sample preparation	28
Purification of the HydA1 protein	28
In vitro reconstitution of the iron-sulfur clusters in the HydA1 _{pur} protein	29
In vitro maturation of the HydA1 _{pur} protein	29
In vitro hydrogenase activity assay	29
Hydrogen measurements by GC	30
EPR measurements	30
Spin quantification	30
EPR simulations	30
References	31

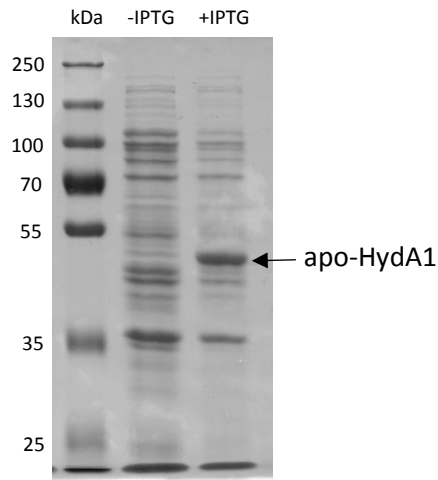


Figure S-1. SDS-PAGE analysis to determine the expression level of the apo-HydA1 protein in M9 minimal media. -IPTG sample collected before IPTG induction, +IPTG sample after 1mM IPTG induction with continuous shaking for 4h at 37°C. The samples loaded on the gel were normalized by OD₆₀₀. The overproduced apo-HydA1 shows up in the +IPTG sample at 49 kDa. As size reference PageRuler Plus Prestained Protein Ladder (ThermoFisher Scientific) was used.

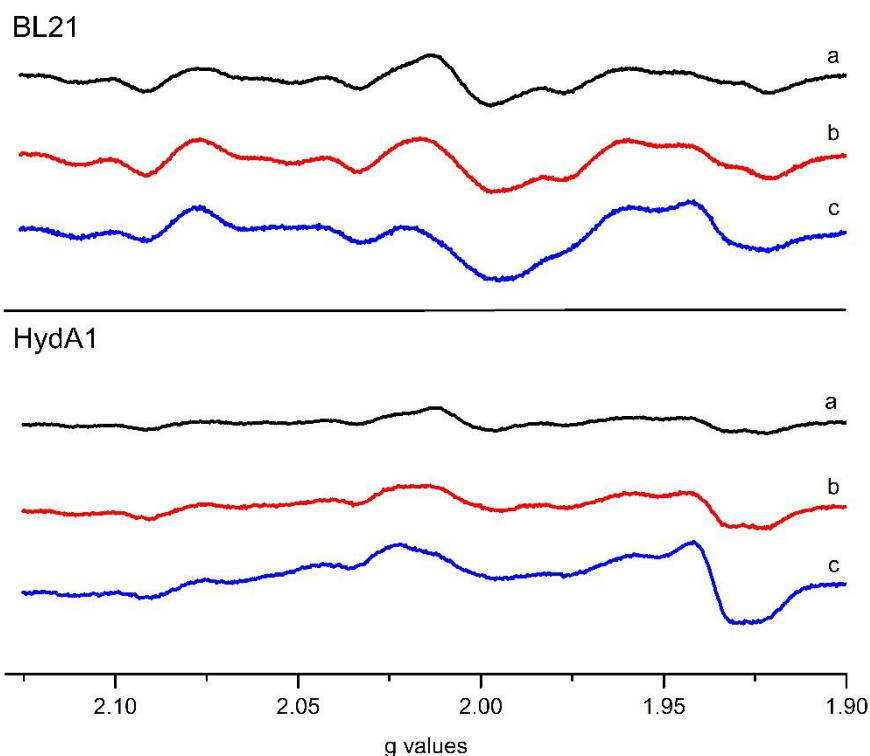


Figure S-2. X-band EPR signals observed for BL21(DE3) cells with and without expression of apo – HydA1, and their respective microwave power dependence. 50 mL BL21(DE3) cell culture concentrated to 200 μ L, either lacking (top) or containing the HydA1 plasmid (bottom). EPR spectra were recorded at 10 K, microwave power: (a) 0.1 mW (b) 1 mW (c) 10 mW; frequency 9.28 GHz, modulation amplitude 1.5 mT, modulation frequency 100 kHz. The different spectra show some preparation dependent differences, but the amplitude of these background signals is negligible compared to the signal intensity of the [2Fe]^{pdt} activated HydA1.

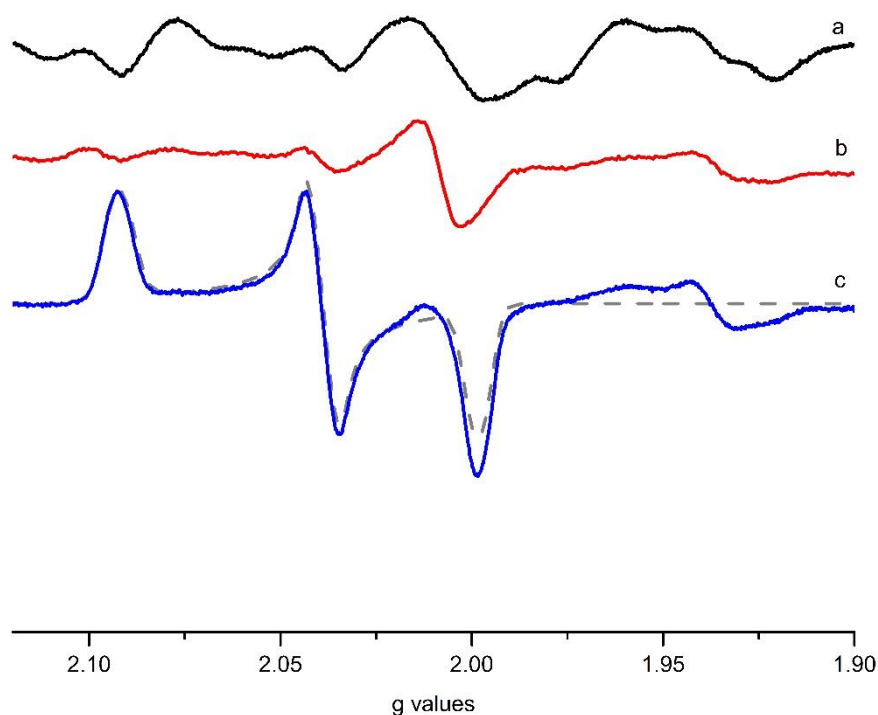


Figure S-3. EPR spectra recorded on whole cell samples of BL21(DE3) not expressing HydA1 incubated with $[2\text{Fe}]^{\text{pdt}}$. 50 mL BL21(DE3) cell cultures concentrated to 200 μL without addition of $[2\text{Fe}]^{\text{pdt}}$ (a); and with addition of 100 μg (156 nmoles) $[2\text{Fe}]^{\text{pdt}}$ (b); The H_{ox} -like $[2\text{Fe}]^{\text{pdt}}$ -HydA1 spectrum (solid line) shown together with the simulated spectrum (dashed line) for reference (c). EPR spectra were recorded at 10 K, microwave power 1 mW, frequency 9.28 GHz, modulation amplitude 1.5 mT, modulation frequency 100 kHz. No features attributable to an H_{ox} -like species was observed in these samples.

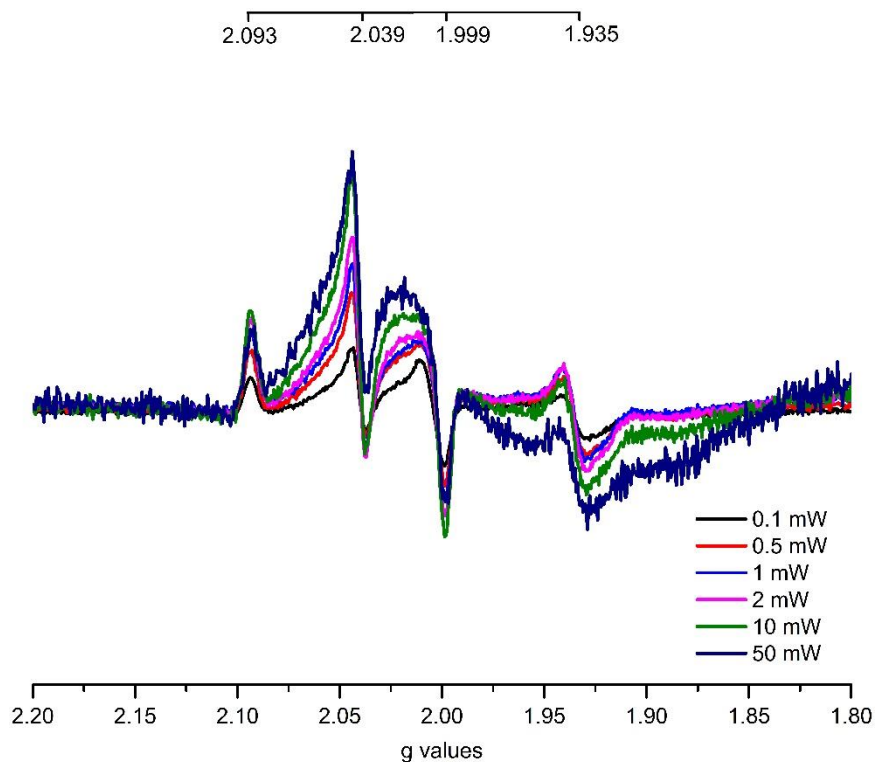


Figure S-4. Microwave power dependence of $[2\text{Fe}]^{\text{pdt}}\text{-HydA1}$ in whole cells at 5 K. EPR spectra were recorded at 5 K on whole cell samples containing $[2\text{Fe}]^{\text{pdt}}\text{-HydA1}$, microwave power 0.1 - 50 mW, frequency 9.28 GHz, modulation amplitude 1.5 mT, modulation frequency 100 kHz.

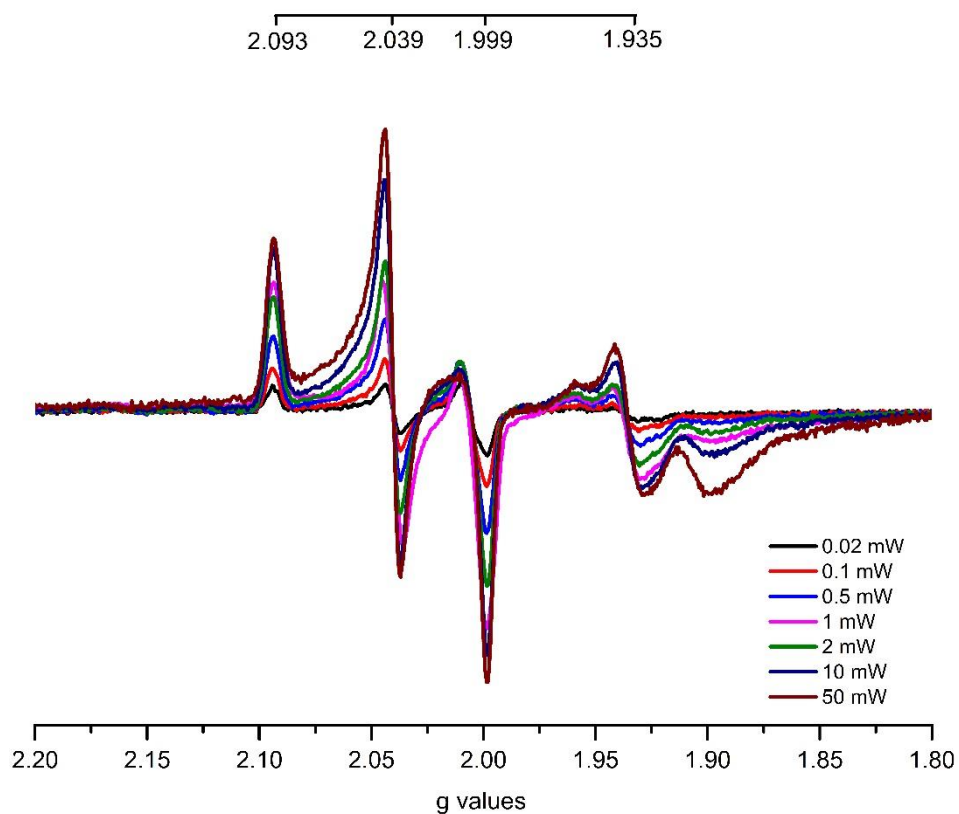


Figure S-5. Microwave power dependence of [2Fe]^{Pdt}-HydA1 in whole cells at 10 K. EPR spectra were recorded at 10 K on whole cell samples containing [2Fe]^{Pdt}-HydA1, microwave power 0.02 - 50 mW, frequency 9.28 GHz, modulation amplitude 1.5 mT, modulation frequency 100 kHz.

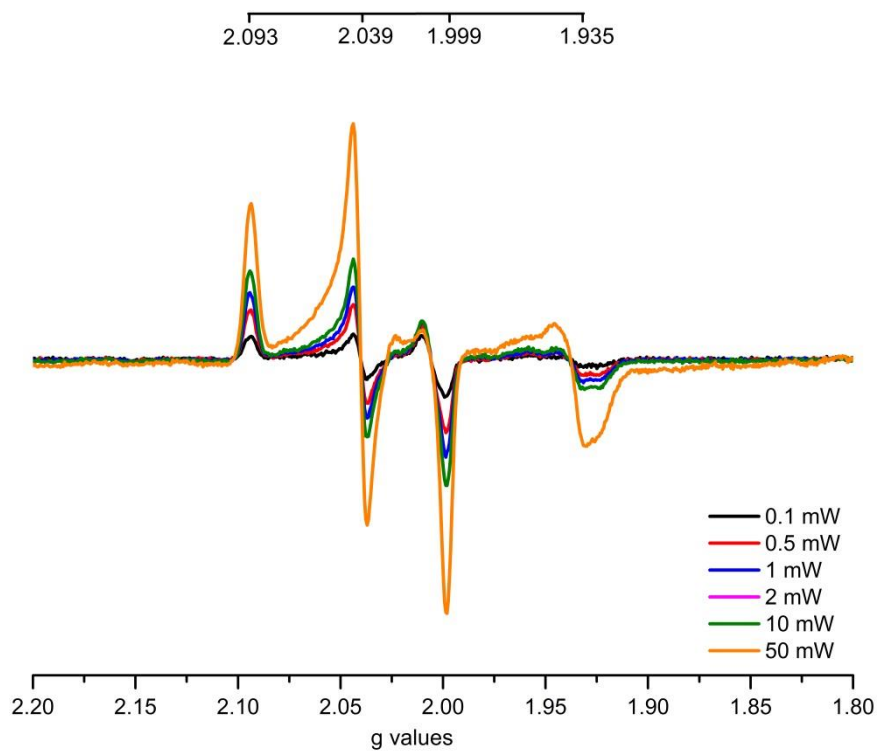


Figure S-6. Microwave power dependence of [2Fe]^{pdT}-HydA1 in whole cells at 20 K. EPR spectra were recorded at 20 K on whole cell samples containing [2Fe]^{pdT}-HydA1, microwave power 0.1 - 50 mW, frequency 9.28 GHz, modulation amplitude 1.5 mT, modulation frequency 100 kHz.

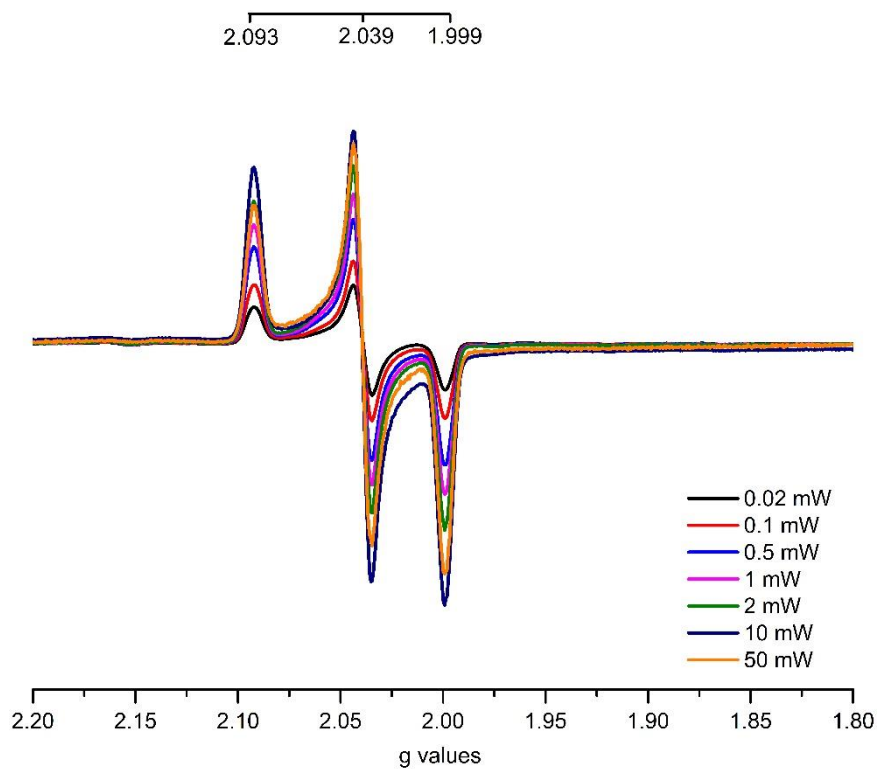


Figure S-7. Microwave power dependence of [2Fe]^{pdt}-HydA1_{pur} at 5 K. EPR spectra were recorded at 5 K on samples of purified enzyme, microwave power 0.02 – 50 mW, frequency 9.28 GHz, modulation amplitude 1.5 mT, modulation frequency 100 kHz.

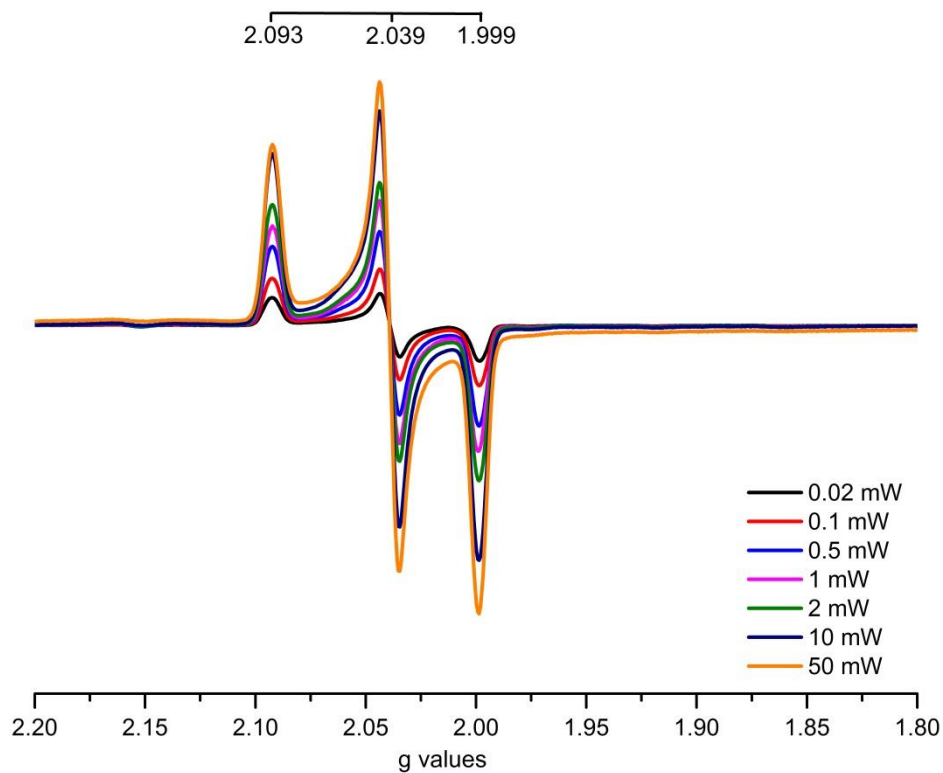


Figure S-8. Microwave power dependence of [2Fe]^{Pdt}-HydA1_{pur} at 10 K. EPR spectra were recorded at 10 K on samples of purified enzyme, microwave power 0.02 – 50 mW, frequency 9.28 GHz, modulation amplitude 1.5 mT, modulation frequency 100 kHz.

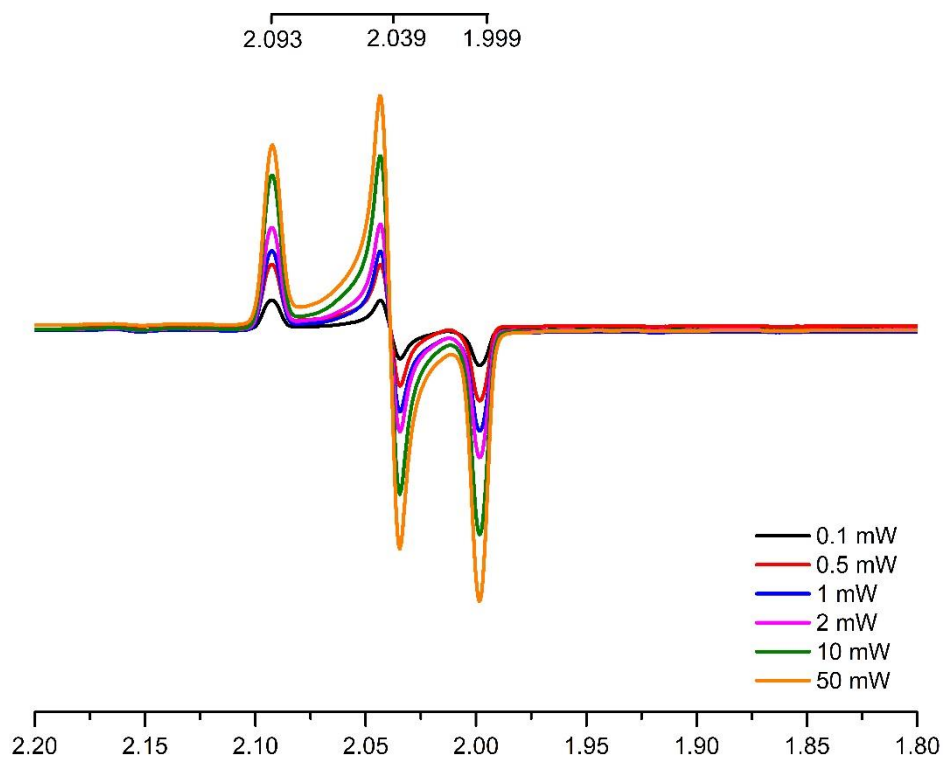


Figure S-9. Microwave power dependence of [2Fe]^{Pdt}-HydA1_{pur} at 20 K. EPR spectra were recorded on samples of purified enzyme at 20 K, microwave power 0.1 – 50 mW, frequency 9.28 GHz, modulation amplitude 1.5 mT, modulation frequency 100 kHz.

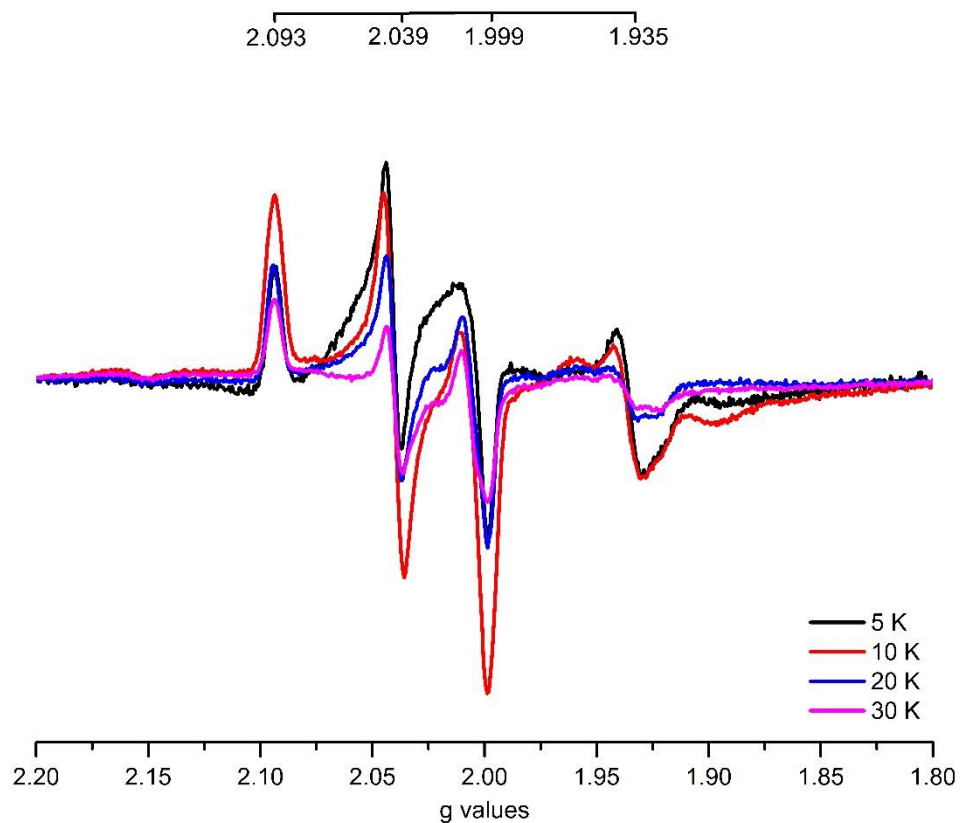


Figure S-10. Temperature dependence of $[2\text{Fe}]^{\text{pdt}}\text{-HydA1}$ in whole cells. EPR spectra were recorded on whole cell samples containing $[2\text{Fe}]^{\text{pdt}}\text{-HydA1}$, between 5 - 30 K, microwave power 1 mW, frequency of 9.28 GHz, modulation amplitude 1.5 mT, modulation frequency 100 kHz.

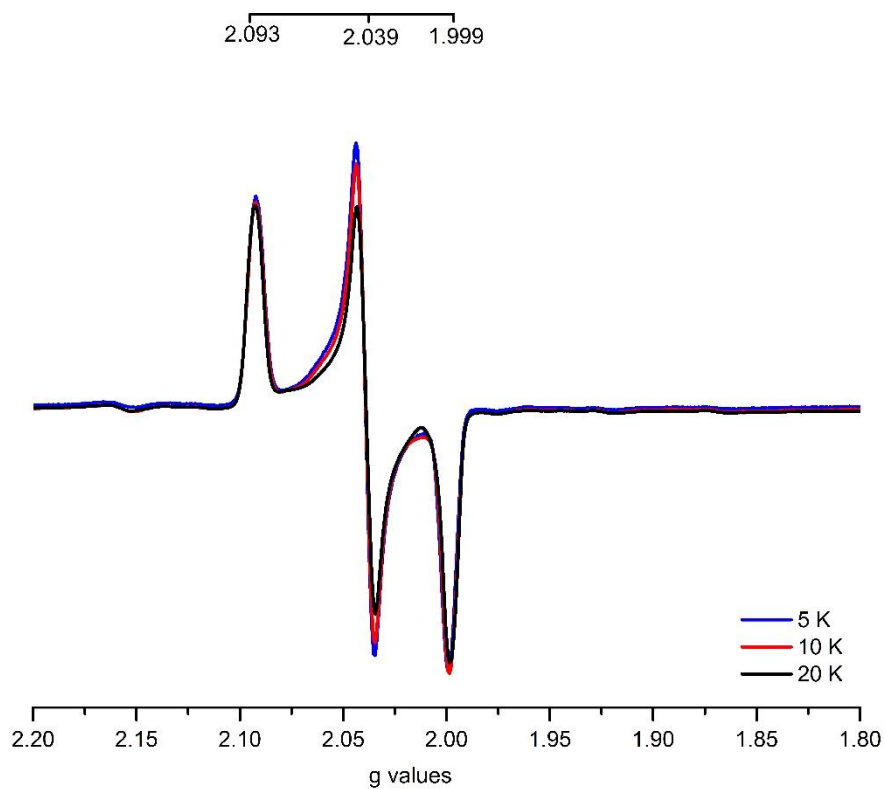


Figure S-11. Temperature dependence of [2Fe]^{pd}-HydA1_{pur}. EPR spectra were recorded at 5 - 20 K on samples of purified enzyme, microwave power 1 mW, frequency of 9.28 GHz, modulation amplitude 1.5 mT, modulation frequency 100 kHz.

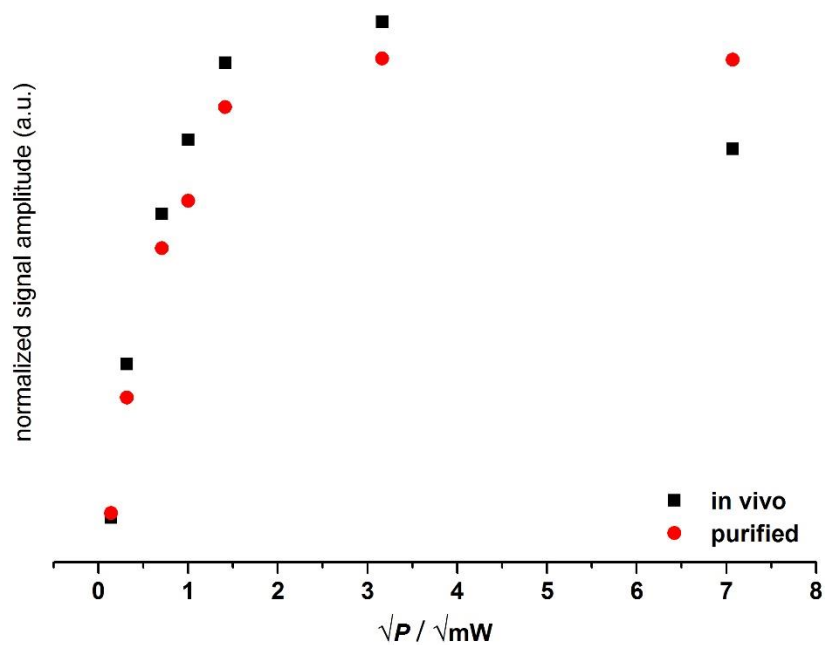


Figure S-12. Microwave power saturation behavior of $[2\text{Fe}]^{\text{pdH}}\text{-HydA1}$ at 5 K. EPR spectra were recorded at 5 K on whole cell samples (black squares) and purified enzyme (red circles), microwave power 0.02 – 50 mW, signal intensity determined by measuring the $g = 2.09$ peak for in vivo and in vitro samples, respectively. The signal amplitudes of the in vitro data was divided by a factor of 9.5 for clarity. Frequency of 9.28 GHz, modulation amplitude 1.5 mT, modulation frequency 100 kHz.

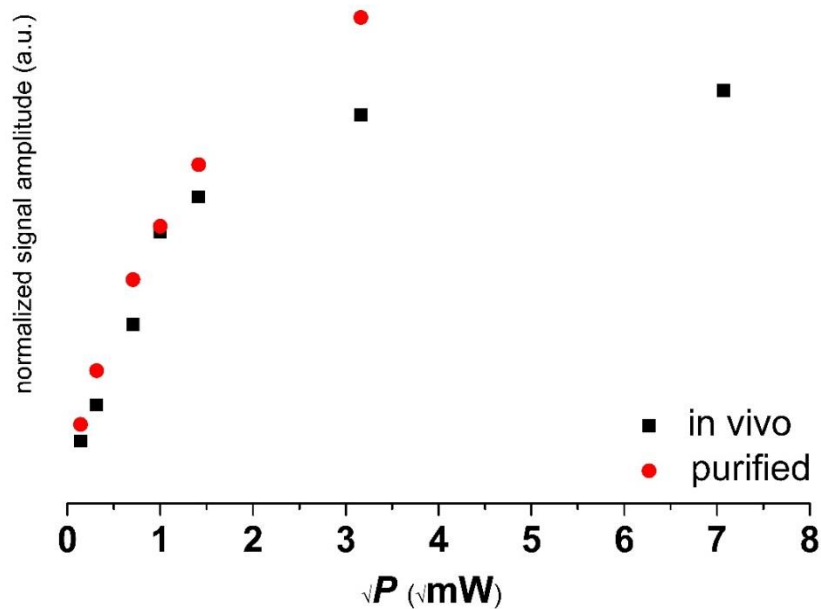


Figure S-13. Microwave power saturation behavior of $[2\text{Fe}]^{\text{Pdt}}\text{-HydA1}$ at 10 K. EPR spectra were recorded at 10 K on whole cell samples (black squares) and purified enzyme (red circles), microwave power 0.02 – 50 mW, signal intensity determined by measuring the $g = 2.09$ peak for in vivo and in vitro samples, respectively. The signal amplitudes of the in vitro data was divided by a factor of 9.5 for clarity. Frequency 9.28 GHz, modulation amplitude 1.5 mT, modulation frequency 100 kHz.

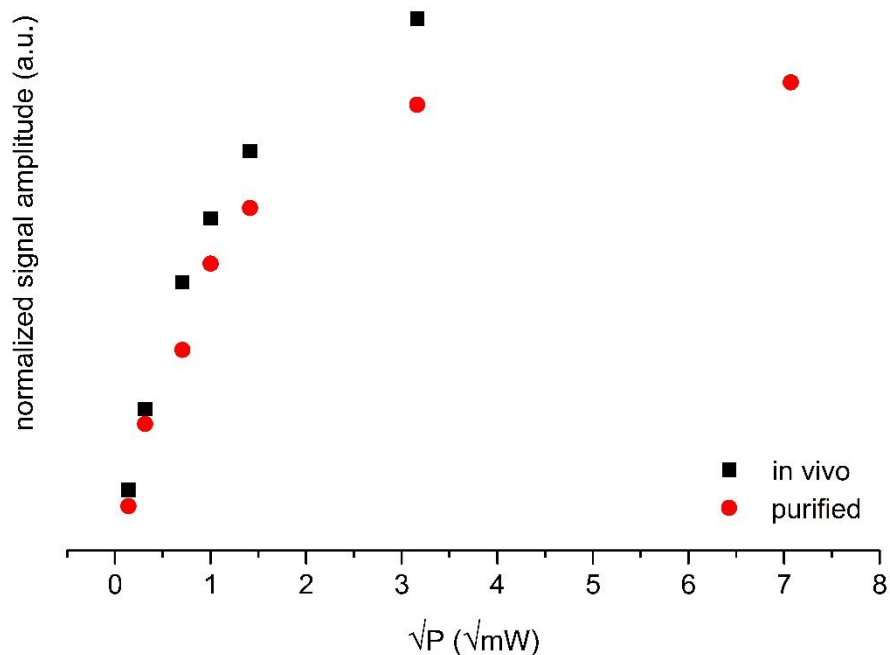


Figure S-14. Microwave power saturation behavior of $[2\text{Fe}]^{\text{pd}}\text{-HydA1}$ at 20 K. EPR spectra were recorded at 20 K on whole cell samples (black squares) and purified enzyme (red circles), microwave power 0.02 – 50 mW, signal intensity determined by measuring the $g = 2.09$ peak for in vivo and in vitro samples, respectively. The signal amplitudes of the in vitro data was divided by a factor of 9.5 for clarity. Frequency 9.28 GHz, modulation amplitude 1.5 mT, modulation frequency 100 kHz.

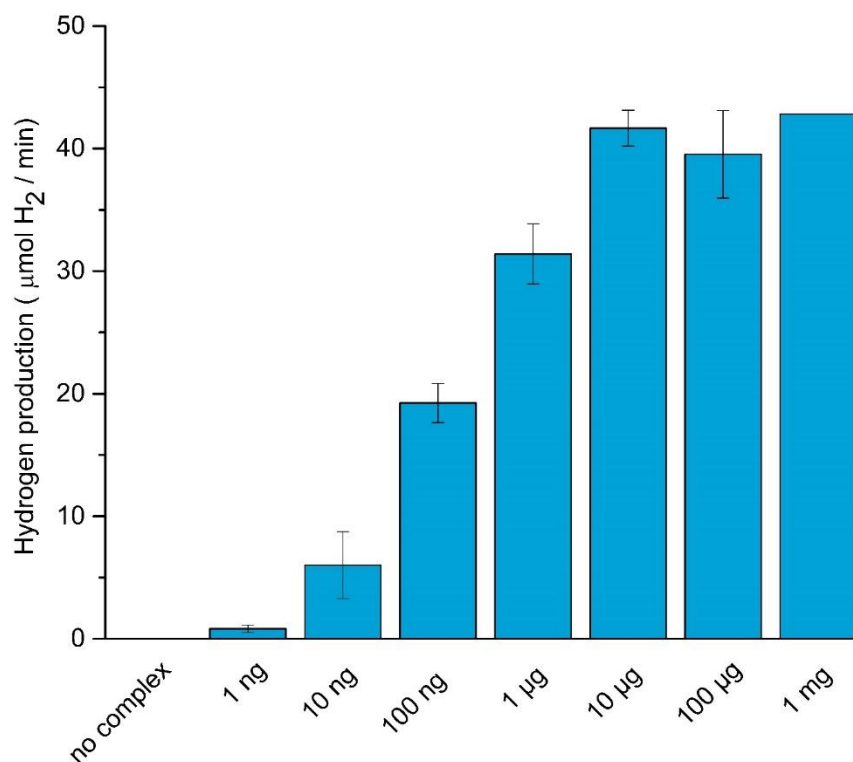


Figure S-15. In vitro hydrogenase activity assay to determine the amount of HydA1 protein available for activation in the cell cultures. BL21(DE3) cells containing the overproduced apo-HydA1 were lysed and the enzyme was activated with 0 – 1 mg (0 – 1.56µmol) [2Fe]^{adt} / 10 mL cell culture. Assay conditions: [MV] = 10 mM, [dithionite] = 20 mM, [kPi] = 60 mM, pH 6.8. The hydrogen production rates were determined by measuring H₂ content in the headspace gas after 15 minutes. All data points excluding the 1 mg addition represent at least two independent repeats with duplicate samples from each culture. Error bars indicate ± standard deviation.

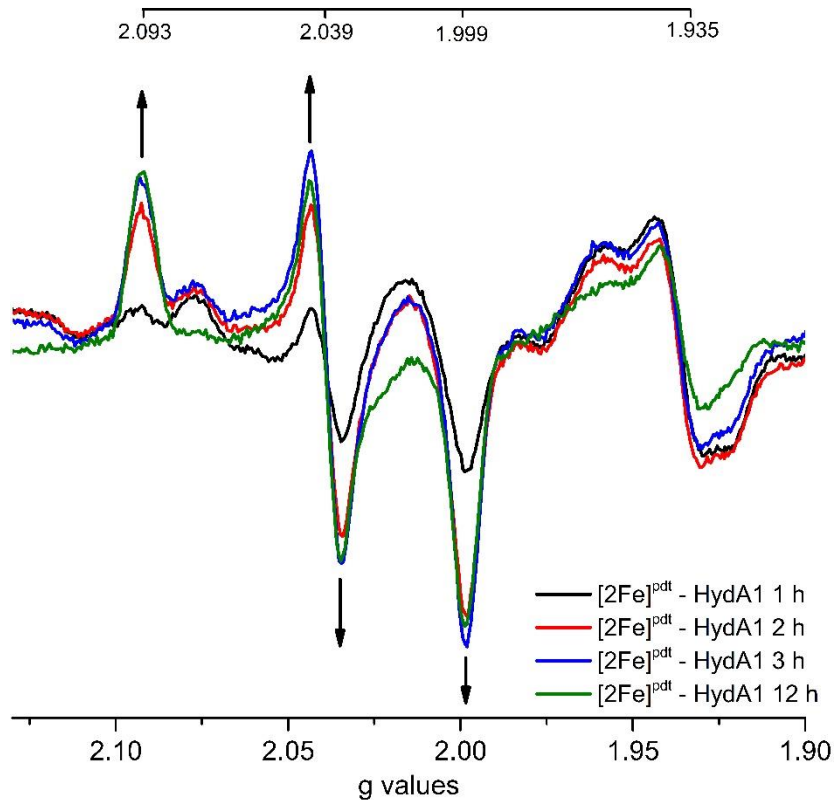


Figure S-16. Formation of [2Fe]^{pdt}-HydA1 under in vivo conditions monitored by EPR spectroscopy. The experiment was performed in an identical fashion to that shown in Figure 3. Samples collected of cells expressing apo-HydA1 after 1, 2, 3 and 12 h of incubation in the presence of [2Fe]^{pdt}, the appearance of the H_{ox}-like signal is indicated with arrows. EPR spectra were recorded at 10 K, microwave power 1mW, frequency 9.28 GHz, modulation amplitude 1.5 mT, modulation frequency 100 kHz.

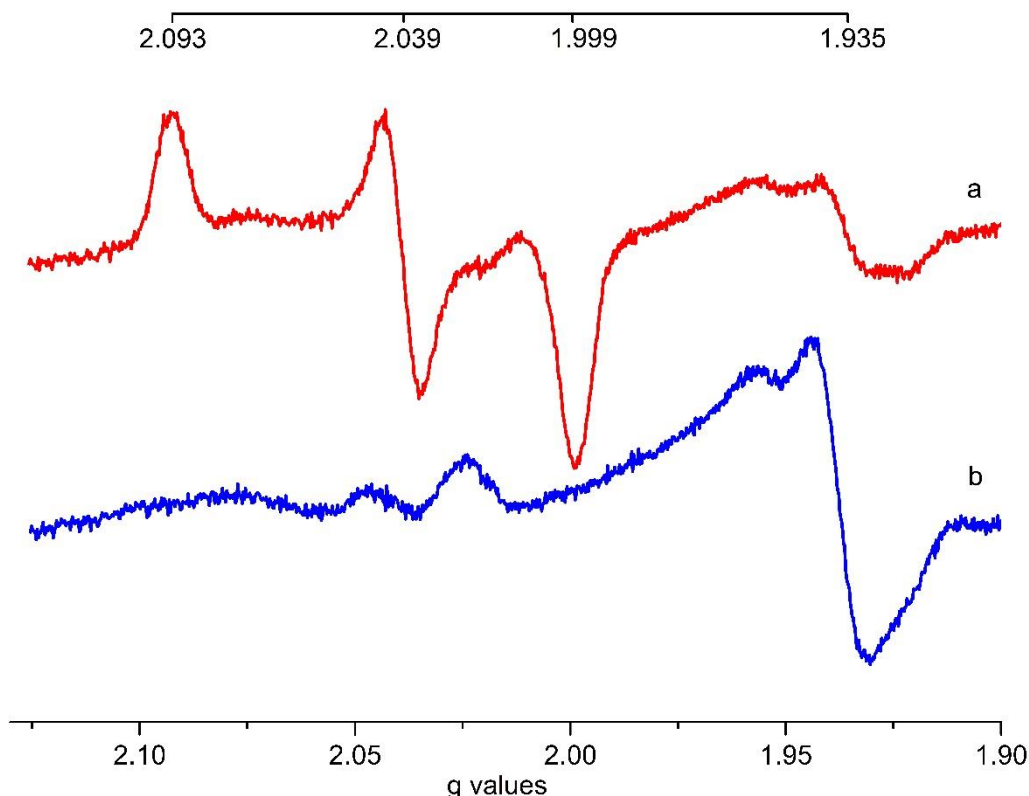


Figure S-17. Reduction of $[2\text{Fe}]^{\text{pdt}}\text{-HydA1}$ after cell lysis. A 50 mL cell culture containing the overproduced apo-HydA1 was activated under in vivo conditions with 100 μg (156 nmoles) $[2\text{Fe}]^{\text{pdt}}$ to form $[2\text{Fe}]^{\text{pdt}}\text{-HydA1}$. Following a 1h incubation in the presence of $[2\text{Fe}]^{\text{pdt}}$, the cells were washed and lysed under anaerobic conditions. One half of the sample was incubated in the glove box for 30 min under argon atmosphere (a); while the other half was incubated with 10 mM Na-dithionite for 30 min under argon atmosphere (b). After the incubation the samples were transferred to EPR tubes and flash frozen. EPR spectra were recorded at 10 K, microwave power 1 mW, frequency 9.28 GHz, modulation amplitude 1.5 mT, modulation frequency 100 kHz. The disappearance of the H_{ox} -like signal is evident upon dithionite reduction and is attributed to the formation of the EPR silent H'_{red} - state ($[\text{4Fe-4S}]^+ - [\text{2Fe(I,II)}]$). The concomitant increase of the feature at $g \approx 1.935$ is tentatively attributed to the formation of reduced $[\text{4Fe4S}]$ clusters present in the host cell.

The absence of new features at $g \approx 2.07\text{-}2.08$ indicates that the system does not proceed to even more reduced states (e.g. $\text{H}_{\text{sred}} [\text{4Fe-4S}]^+ - [\text{2Fe(I,I)}]$ or $\text{H}_{\text{Hyd}} [\text{4Fe-4S}]^+ - [\text{2Fe(II,II)}](\text{H}^-)$). This observation is in agreement with earlier in vitro spectroscopic studies of $[2\text{Fe}]^{\text{pdt}}\text{-HydA1}$.^[1]

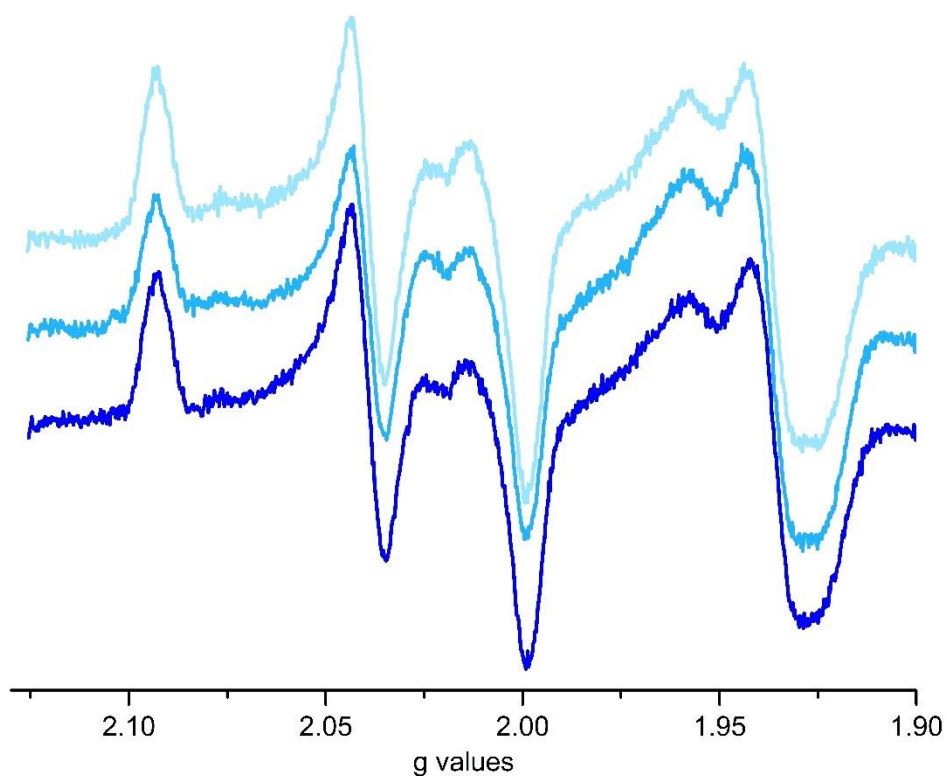


Figure S-18. Stability of $[2\text{Fe}]^{\text{pdT}}\text{-HydA1}$ in an H_{ox} -like state under in vivo conditions. Apo-HydA1 expressing cells were incubated with $[2\text{Fe}]^{\text{pdT}}$ for one hour, after which unreacted complexes were removed via centrifugation and washing of the cells as previously described.^[2] Whole cell EPR spectra of $[2\text{Fe}]^{\text{pdT}}\text{-HydA1}$ recorded on cell cultures stored under argon atmosphere for: (a) 30 min (b) 60 min (c) 180 min.

Subsequent incubation of the washed $[2\text{Fe}]^{\text{pdT}}$ treated cells for 3h under an argon atmosphere did not result in significant change to the EPR spectra, suggesting that the equilibrium does not change on the time-scale of our experiments.

EPR spectra were recorded at 10 K, microwave power 1 mW, frequency 9.28 GHz, modulation amplitude 1.5 mT, modulation frequency 100 kHz.

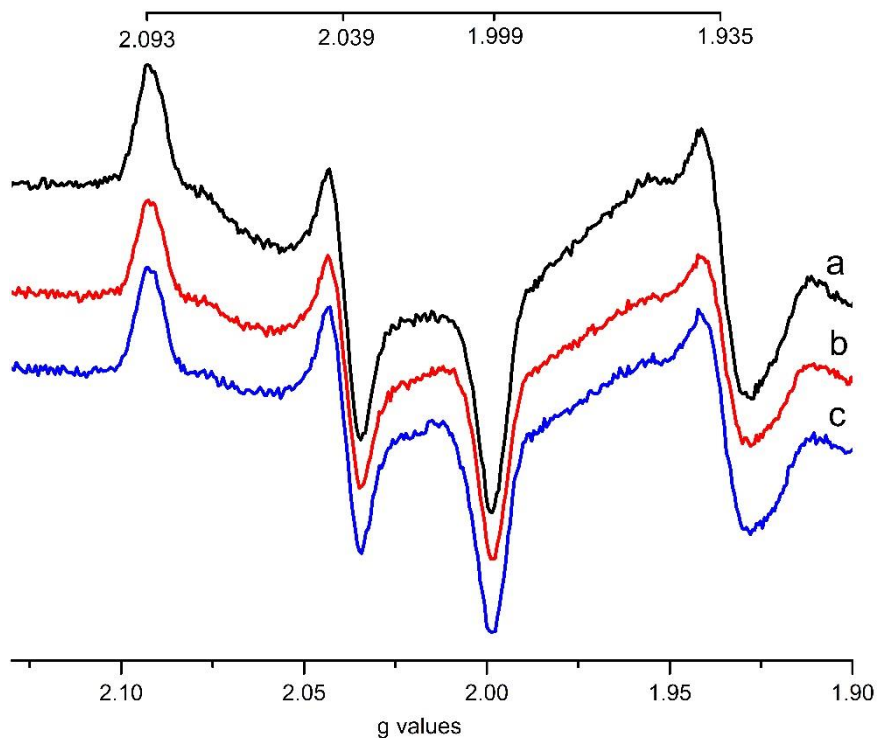


Figure S-19. $[2\text{Fe}]^{\text{pdT}}\text{-HydA1}$ oxidation under in vivo conditions. A 50 mL cell culture containing the overproduced apo-HydA1 was activated in vivo with 100 μg (156 nmoles) $[2\text{Fe}]^{\text{pdT}}$ to form $[2\text{Fe}]^{\text{pdT}}\text{-HydA1}$. The cells were washed three times with TRIS buffer (100 mM TRIS pH 7.5, 150 mM NaCl) concentrated to 200 μL and incubated in different ways: (a) Ar atmosphere in the glove box for 30 min, (b) air for 30 min, (c) Ar atmosphere in the glove box in the presence of 3 mM potassium - ferricyanide for 30 min. After the incubation, the cells were frozen in EPR tubes. Further oxidation of the $2\text{Fe}]^{\text{pdT}}\text{-HydA1}$ via incubation of the cell cultures in air or using chemical oxidation with ferricyanide did not cause any significant change in the signal. Likewise, treating the cells with dithionite or flushing the headspace with H_2 for one hour before freezing did not appear to influence the redox state of the H-cluster (data not shown).

EPR spectra were recorded at 10 K, microwave power 1 mW, frequency 9.28 GHz, modulation amplitude 1.5 mT, modulation frequency 100 kHz.

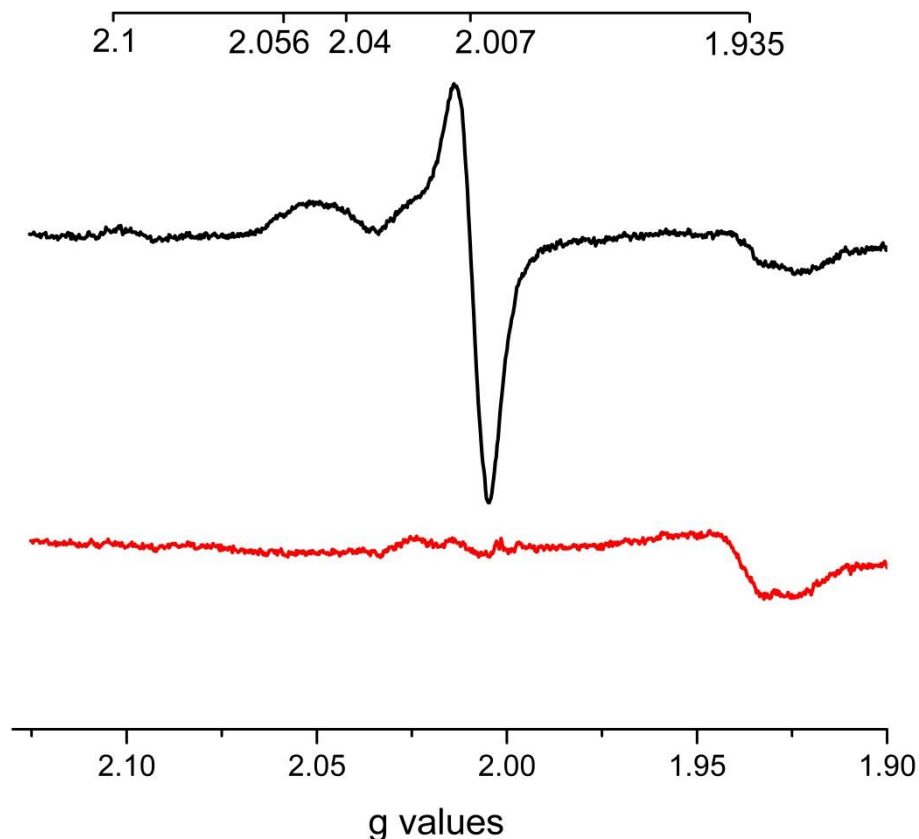


Figure S-20. Reduction of $[2\text{Fe}]^{\text{adt}}\text{-HydA1}$ after cell lysis. A 50 mL cell culture containing the overproduced apo-HydA1 was activated under in vivo conditions with 100 μg (156 nmoles) $[2\text{Fe}]^{\text{adt}}$ to form $[2\text{Fe}]^{\text{adt}}\text{-HydA1}$. Following a 1h incubation in the presence of $[2\text{Fe}]^{\text{adt}}$, the cells were washed and lysed under anaerobic conditions. One half of the sample was incubated in the glove box for 30 min under argon atmosphere (black line); while the other half was incubated with 10 mM Na-dithionite for 30 min under argon atmosphere (red line). After the incubation the samples were transferred to EPR tubes and flash frozen. EPR spectra were recorded at 20 K, microwave power 1 mW, frequency 9.28 GHz, modulation amplitude 1.5 mT, modulation frequency 100 kHz. The disappearance of the signals attributed to H_{ox} and $\text{H}_{\text{ox}}\text{-CO}$ is evident upon dithionite reduction; the concomitant increase of the feature at $g \approx 1.935$ is tentatively attributed to the formation of reduced $[\text{4Fe4S}]$ clusters present in the host cell.

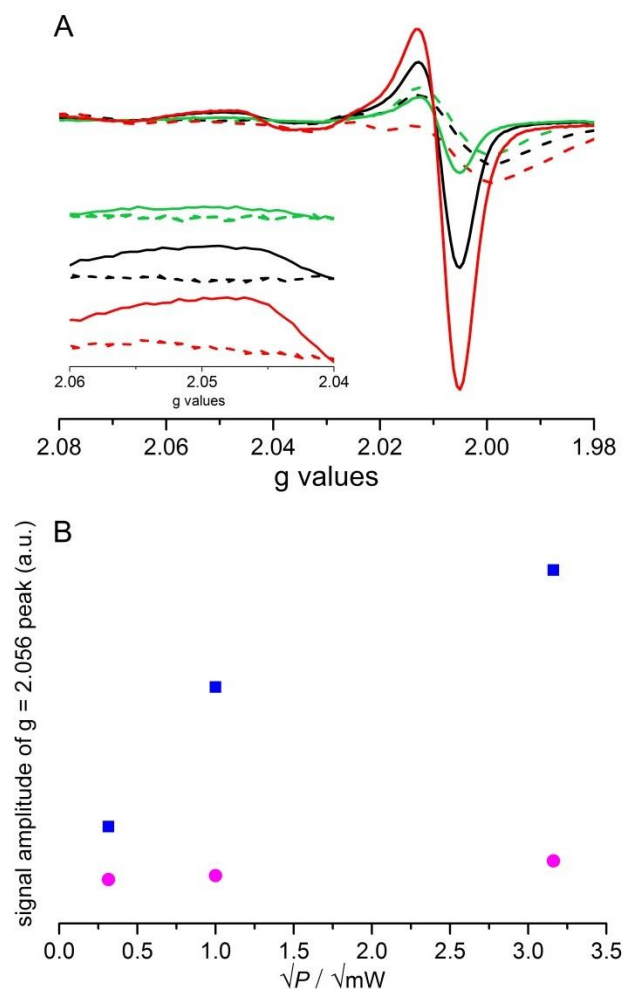


Figure S-21. Comparison of the microwave power dependence in the $\text{H}_{\text{ox}}\text{-CO}$ signal region in cells containing or not containing the fully assembled $[\text{2Fe}]^{\text{adt}}\text{-HydA1}$ cluster (studied at 20K). (A): EPR spectra of whole cell samples expressing the apo-HydA1 enzyme (solid lines) compared to cell samples not expressing the apo-HydA1 enzyme (dashed lines). Both cells types were treated with $[\text{2Fe}]^{\text{adt}}$, and measured at different microwave powers (red: 10 mW; black: 1 mW; green: 0.1 mW). The inset shows the amplified $\text{H}_{\text{ox}}\text{-CO}$ fingerprint region at $g = 2.05$. (B) Microwave power dependence of the $g = 2.056$ signal in (A) (blue squares: whole cell samples expressing the apo-HydA1 enzyme; purple circles: whole cells not expressing the apo-HydA1 enzyme), showing the higher relaxation rate for cells containing the fully assembled H-cluster.

Spectra recorded at 20 K, microwave frequency of 9.28 GHz, modulation amplitude 1.5 mT, modulation frequency 100 kHz.

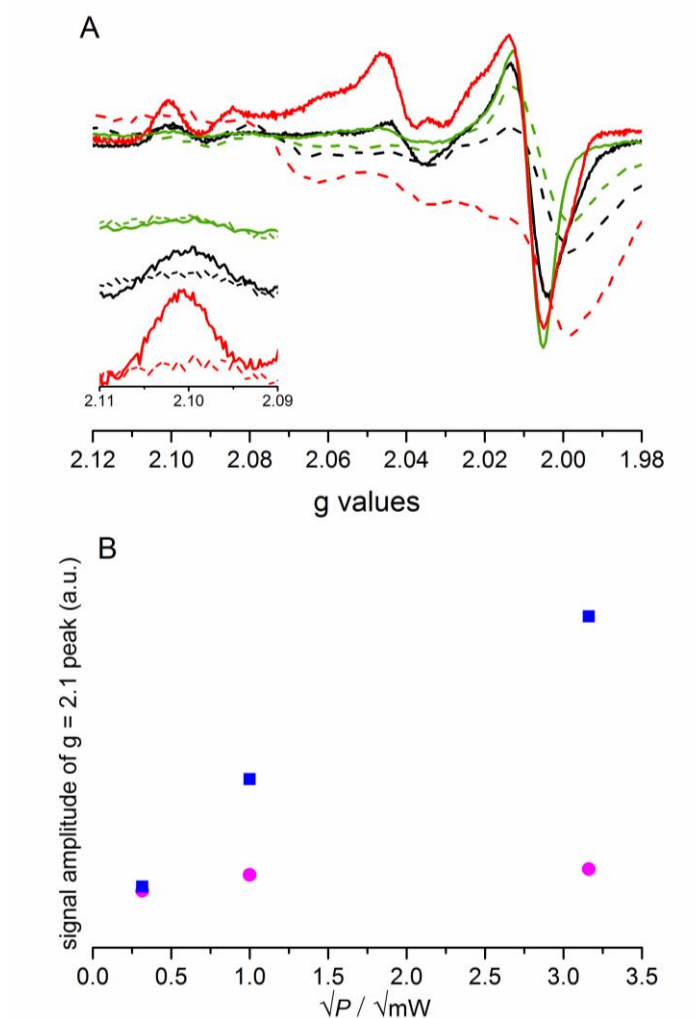


Figure S-22. Comparison of the microwave power dependence behavior in the H_{ox} signal region in cells containing or not containing the fully assembled $[2Fe]^{adt}$ -HydA1 cluster (studied at 10K). (A): EPR spectra of whole cell samples expressing the apo-HydA1 enzyme (solid lines) compared to cell samples not expressing the apo-HydA1 enzyme (dashed lines). Both cells types were treated with $[2Fe]^{adt}$, and measured at different microwave powers (red: 10 mW; black: 1 mW; green: 0.1 mW). The inset shows the amplified H_{ox} fingerprint region at $g = 2.10$. (B) Microwave power dependence of the $g = 2.100$ signal in (A) (blue squares: whole cell samples expressing the apo-HydA1 enzyme; purple circles: whole cells not expressing the apo-HydA1 enzyme), showing the higher relaxation rate for cells containing the fully assembled H-cluster.

Spectra recorded at 10 K, microwave frequency of 9.28 GHz, modulation amplitude 1.5 mT, modulation frequency 100 kHz.

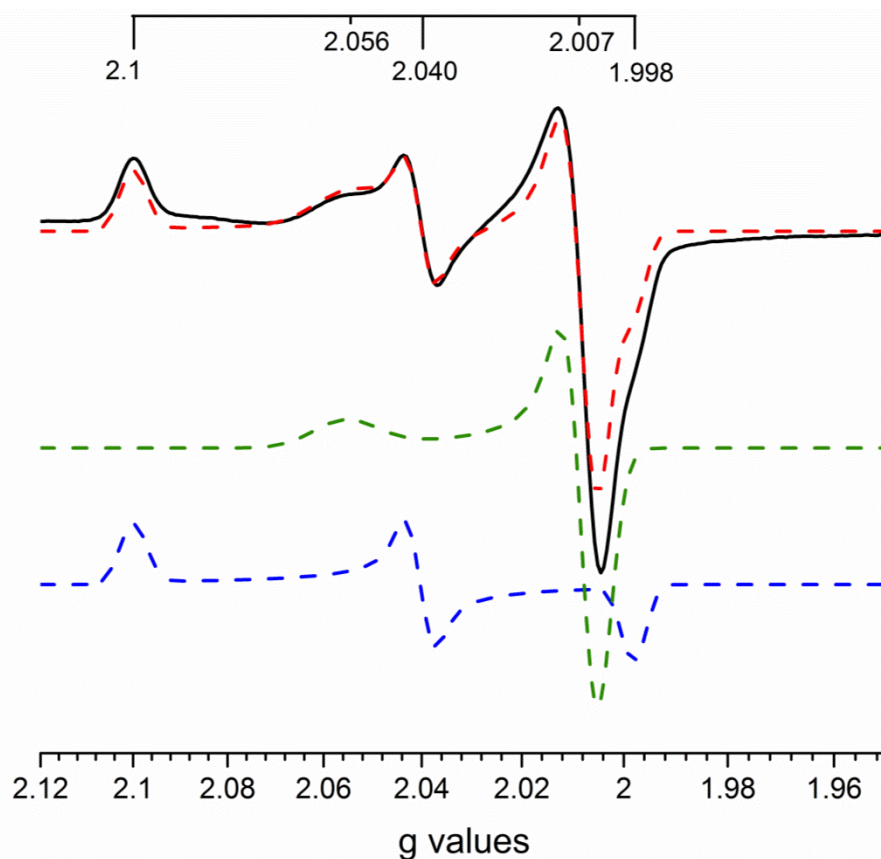


Figure S-23. Simulation of the EPR spectrum of $[2\text{Fe}]^{\text{adt}}\text{-HydA1}_{\text{pur}}$ recorded at 10K. The spectrum of thionine oxidized $[2\text{Fe}]^{\text{adt}}\text{-HydA1}_{\text{pur}}$ featuring a mixture of the H_{ox} and $\text{H}_{\text{ox}}\text{-CO}$ states (black solid line), as previously observed for thionine treated samples of $[2\text{Fe}]^{\text{adt}}\text{-HydA1}$ ^[3]. Overlaid on the spectrum is the simulation generated from a combination of H_{ox} (60%) and $\text{H}_{\text{ox}}\text{-CO}$ (40%) (red dashed line). Simulations of the pure species are displayed in green ($\text{H}_{\text{ox}}\text{-CO}$; $g = 2.056$ 2.007 2.007) and blue (H_{ox} ; $g = 2.100$, 2.040 , 1.998).

EPR spectra recorded at 10 K, microwave power 1 mW, frequency 9.28 GHz, modulation amplitude 1 mT, modulation frequency 100 kHz. Simulations were carried out using the easyspin toolbox in Matlab (see experimental section).

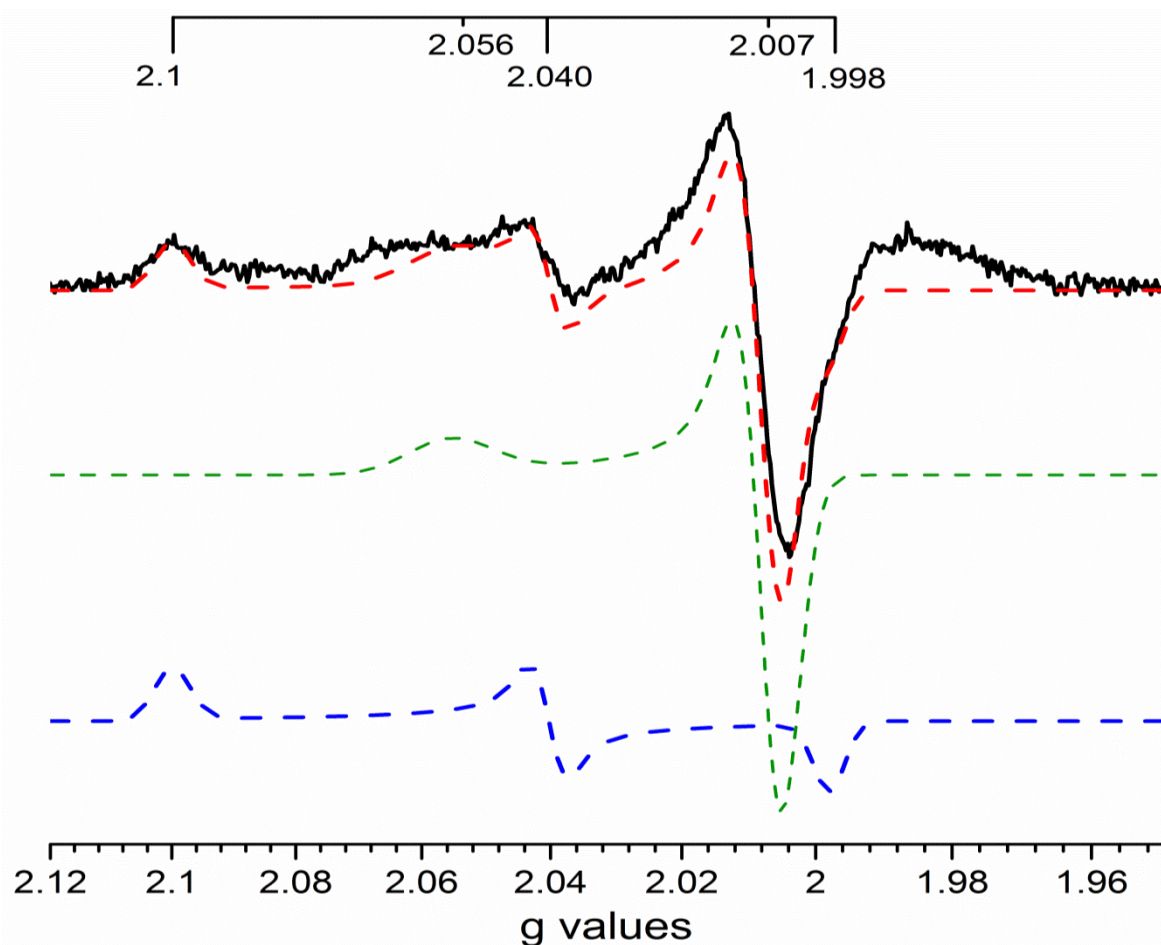


Figure S-24. Simulation of the EPR spectrum of $[2\text{Fe}]^{\text{adt}}\text{-HydA1}$ in whole cells recorded at 10K. The background subtracted spectrum observed for $[2\text{Fe}]^{\text{adt}}\text{-HydA1}$ in whole cells (black line, identical to spectrum d in Figure 4). Overlaid on the spectrum is the simulated spectrum generated from a combination of H_{ox} (40%) and $\text{H}_{\text{ox-CO}}$ (60%) (red dashed line). Simulated spectra of the pure species are displayed in green ($\text{H}_{\text{ox-CO}}$; $g = 2.056\ 2.007\ 2.007$) and blue (H_{ox} ; $g = 2.100, 2.040, 1.998$). Apart from the signal amplitude and $\text{H}_{\text{ox-CO}}/\text{H}_{\text{ox}}$ ratio no parameters were changed in the simulation between in vitro and in vivo conditions.

EPR spectra recorded at 10 K, microwave power 1 mW, frequency 9.28 GHz, modulation amplitude 1 mT, modulation frequency 100 kHz. Simulations were carried out using the easyspin toolbox in Matlab (see experimental section).

Table S-1. Simulation parameters of the $\text{H}_{\text{ox}}\text{-[2Fe]}^{\text{pdt}}$ (= H_{ox} -like), H_{ox} and $\text{H}_{\text{ox}}\text{-CO}$ species. Simulations are presented in figures 2, 4, S-3, S-23 and S-24. The line width parameter H_{strain} is expressed in mT.

Species	$g_z (\text{H}_{\text{strain}})$	$g_y (\text{H}_{\text{strain}})$	$g_x (\text{H}_{\text{strain}})$
$\text{H}_{\text{ox}}\text{-[2Fe]}^{\text{pdt}}$	2.093 (1)	2.039 (0.68)	1.999 (0.8)
H_{ox}	2.100 (0.85)	2.040 (0.67)	1.998 (0.68)
$\text{H}_{\text{ox}}\text{-CO}$	2.056 (2.5)	2.007 (1.25)	2.007 (1.25)

Table S-2. Comparison of the g values observed in this work with the previous literature data.

H-cluster state	g_z	g_y	g_x	Reference
H_{ox} native	2.100	2.037	1.996	[4]
	2.102	2.040	1.998	[5]
	2.100	2.039	1.997	[3]
H_{ox} [2Fe] ^{adt}	2.100	2.040	1.998	This paper
H_{ox} [2Fe] ^{pd}	2.094	2.039	1.998	[1]
H_{ox} [2Fe] ^{pd}	2.093	2.039	1.999	This paper
H_{ox} - CO native	2.052	2.007	2.007	[4-5]
	2.045	2.007	2.007	[3]
H_{ox} -CO [2Fe] ^{adt}	2.056	2.007	2.007	This paper

Experimental Section

General – All chemicals were purchased from Sigma-Aldrich or VWR and used as received unless otherwise stated. Protein content was analyzed by 10% SDS- PAGE minigels in a SE250 Mighty Small II unit (Hoefer) system. The proteins were stained with Page Blue protein staining solution (Thermo Fisher Scientific) according to the supplier's instructions. All anaerobic work was performed in an MBRAUN glovebox ($[O_2] < 10$ ppm). The expression vectors coding the *csdA* and *hydA1* genes respectively were kindly provided by Prof. Marc Fontecave (College de France, Paris/CEA, Grenoble). The His-tagged CsdA enzyme was purified following a literature procedure^[6]. The EPR spectra shown are representative signals from at least two individual experiments. The individual experiments show some preparation dependent differences, but the amplitude of these background signals are negligible compared to the signal intensity of the $[2Fe]^{pdt}$ activated HydA1.

Synthesis of $(Et_4N)_2[Fe_2(pdt)(CO)_4(CN)_2]$ ($[2Fe]^{pdt}$) and $(Et_4N)_2[Fe_2(adt)(CO)_4(CN)_2]$ ($[2Fe]^{adt}$) The complexes were synthesized in accordance to literature protocols with minor modifications, and verified by FTIR spectroscopy^[7-10] The complex was dissolved in anaerobic potassium phosphate buffer (100 mM, pH 6.8) at 1 $\mu\text{g}/\mu\text{L}$ concentration and used directly.

Overexpression of the apo-HydA1 hydrogenase - *E. coli* BL21 (DE3) cells containing the HydA1 plasmid were grown in 50 mL M9 medium [22 mM Na_2HPO_4 , 22 mM KH_2PO_4 , 85 mM NaCl, 18 mM NH_4Cl , 0.2 mM MgSO_4 , 0.1 mM CaCl_2 , 0.4% (v/v) glucose] under aerobic conditions until O.D.₆₀₀=0.4 in the presence of antibiotics. The protein overproduction was induced with 1mM IPTG and persisted at 37°C for 4h with continuous aeration. Final O.D.₆₀₀ of the cultures were 0.8 ± 0.2 .

In vivo formation of $[2Fe]^{pdt}$ - and $[2Fe]^{adt}$ -HydA1 – The preparation of the semi-synthetic hydrogenase was performed following a literature protocol with minor modifications.^[2] The apo-HydA1 protein was expressed in 50 ml *E. coli* cultures as described in the *Overexpression of the apo-HydA1 hydrogenase* section. After the 4h expression period the cells were harvested, deaerated and transferred to the glove-box. The cells were re-suspended in fresh M9 medium (2 mL final volume), and formation of $[2Fe]^{pdt}$ - or $[2Fe]^{adt}$ -HydA1 was achieved by treating the cell cultures with 100 μg (156 nmoles) of $[2Fe]^{pdt}$ or $[2Fe]^{adt}$ at 37°C under strict anaerobic conditions.

Whole cell EPR sample preparation – Cell cultures containing the overproduced and activated HydA1 protein were harvested and washed with Tris buffer (100 mM Tris, 150 mM NaCl pH 7.5) three times under anaerobic conditions. The cell paste was diluted to 200 μL with washing buffer and transferred into EPR tubes. The tubes were capped and directly frozen in liquid nitrogen. For the crude extract samples the cells were harvested and treated with 200 μL of anaerobic lysis buffer [60 mM potassium phosphate buffer, pH 6.8, 0.6 mg / mL lysozyme, and 0.2 % (v/v) Triton X-100] following the *in vivo* activation and washing protocol. The cells were then transferred to 2 mL gas tight vials, sealed and lysed by 3 freeze-thaw cycles in an ethanol/dry ice bath. In case of the dithionite reduced samples the crude cell extract was incubated with 10 mM Na-dithionite for 30 minutes.

Purification of the HydA1 protein - His-tagged apo-HydA1 was isolated via a modified literature protocol to generate $\text{HydA1}_{\text{pur}}$.^[11] BL21(DE3) competent cells were transformed with the pET-DUET-CrHydA1 expression vector and positive clones were selected based on

ampicillin resistance. Preparative scale expression was performed in LB medium complemented with 25 mM potassium phosphate buffer pH 7.6 and 5% glucose. When $OD_{600} = 0.4 - 0.6$ was reached, the cultures were transferred to 16°C and the protein expression was induced using 1 mM IPTG. After 12-16 h protein overproduction the cells were harvested by centrifugation and the cell paste was re-suspended in 100 mM HEPES pH 7.4, 300 mM NaCl, 10 mM MgCl₂, 5% glycerol. The suspension was centrifuged and the cell paste was flash frozen in liquid nitrogen, and stored at -80°C. The cell paste was thawed and re-suspended in 100 mM HEPES pH 7.4, 300 mM NaCl, 10 mM MgCl₂, 5% glycerol, complemented with lysozyme, DNase and RNase, and freeze-thawed at least 3 times. The semi-lyzed cells were sonicated and the supernatant was isolated by ultracentrifugation (55000 rpm 60 min 4°C). The resulting supernatant was loaded onto a Ni-NTA (HisTrap) column which was previously equilibrated with 100 mM HEPES pH 7.4, 300 mM NaCl, 10 mM MgCl₂, 5% glycerol. The column was washed with equilibration buffer until the UV absorbance reached the baseline. To eliminate unspecifically bound proteins the column was washed the equilibration buffer complemented with 50 mM imidazole, and when the absorbance reached the baseline again, a 10 column volume 10-100% linear gradient elution was performed (elution buffer composition: 100 mM HEPES pH 7.4, 300 mM NaCl, 10 mM MgCl₂, 5% glycerol and 500 mM imidazole). The imidazole was removed and the protein was concentrated using 30 kDa centricons (Merck). The purity of the protein was verified by SDS-PAGE.

In vitro reconstitution of the iron-sulfur clusters in the HydA_{pur} protein – The metal-free form of HydA_{pur} was generated by incubating the purified protein with 10 mM EDTA in the presence of reducing agent (20 mM Na-dithionite) under strict anaerobic conditions for 1-2 hours at 4°C. To separate the chelated metal ions from the protein, the protein was purified using a Superdex 200. The column was equilibrated with 100 mM Tris-HCl pH 8.0, 300 mM NaCl, 10 mM MgCl₂ and 5% glycerol before usage. Following the demetallization treatment the [4Fe4S] cluster was reconstitution under strict anaerobic conditions. The protein sample was equilibrated 1-2 hours at 4°C inside a glovebox atmosphere, then it was incubated with tenfold molar excess of DTT for 10-15 minutes at room temperature. The DTT incubation was followed by the addition of sixfold molar excess of ferrous ammonium sulfate and sixfold molar excess of L-cysteine. The reconstitution reaction was initiated by the addition of 1-2% molar equivalent of CsdA enzyme (cysteine desulfurase from *E.coli*). The reaction was followed by observing the increase of absorbance at 400 nm by UV/Visible spectroscopy, when the absorbance reached a plateau it was stopped by running the reaction mixture through a NAP25 desalting column. The protein containing elution fractions were pooled and concentrated using 30 kDa centricons. The protein was aliquoted, flash frozen in liquid nitrogen and stored at -80°C until further usage.

In vitro maturation of the HydA_{pur} protein and preparation of the HydA_{pur} EPR reference sample - The reconstituted HydA_{pur} protein was incubated with twentyfold molar excess of sodium dithionite and twelvefold molar excess of either the [2Fe]^{pd} or the [2Fe]^{adt} complex for 90 minutes at room temperature under low light and strict anaerobic conditions. The maturation reaction was stopped by running the reaction mixture through a NAP 25 desalting column, and the protein containing elution fractions were pooled and concentrated using 30 kDa centricons. 200 µL 100 µM [2Fe]^{pd}-HydA_{pur} or [2Fe]^{adt}-HydA_{pur} was titrated with thionine until the oxidized thionine peaks appeared in the UV/Vis spectrum. The fully oxidized protein solutions was transferred into EPR tubes and flash frozen.

In vitro hydrogenase activity assay - The assay was performed following a slightly modified literature protocol.^[12] 10 mL cultures were harvested after the overexpression of the apo-HydA1 protein as described above, sparged with argon for 10 min and treated with 300 µL of

anaerobic lysis buffer (60 mM potassium phosphate buffer, pH 6.8; 0.6 mg / mL lysozyme, and 0.2 % Triton X-100) inside the glovebox. The cells were then transferred to 2 mL gas tight vials, sealed and lysed by 3 freeze-thaw cycles in an ethanol/dry ice bath. The cell lysate was transferred into 8 mL gas tight glass vials and the appropriate amount of $[2\text{Fe}]^{\text{adt}}$ was added from a stock solution in potassium phosphate buffer (100 mM, pH 6.8). The samples were diluted in 1.42 mL assay buffer (84.5 mM potassium phosphate buffer, pH 6.8, 1.4 % Triton X-100 and 14 mM methyl viologen, final concentration: $[\text{MV}] = 10 \text{ mM}$, $[\text{kPi}] = 60 \text{ mM}$, pH 6.8), and the samples were then sealed and incubated at room temperature for 10 min. Thereafter the reaction was initiated by adding 200 μL of 0.2 M sodium dithionite (final concentration 20 mM). The reactions were incubated at 37 °C using a water bath. The evolution of hydrogen was first recorded after 15 min by injecting 100 μL of the headspace into a gas chromatograph followed by subsequent samples every 30 min. Rates were converted to enzyme content based on a specific activity of $730 \mu\text{mol H}_2 \cdot \text{min}^{-1} \cdot \text{mg}_{\text{HydA1}}^{-1}$ and a molecular weight of HydA1 of 49 kDa.^[2, 5, 13]

Hydrogen measurements by GC - Hydrogen content was determined using a gas chromatograph (GC; PerkinElmer LLC, MA, USA) equipped with a thermal conductivity detector (TCD) and a stainless-steel column packed with Molecular Sieve (60/80 mesh). A calibration curve was established by injecting known amounts of hydrogen. The operational temperatures of the injection port, the oven and the detector were 100 °C, 80 °C and 100 °C, respectively. Nitrogen was used as the carrier gas at a flow rate of 35 mL min⁻¹.

EPR measurements - Measurements were performed on a Bruker ELEXYS E500 spectrometer using an ER049X SuperX microwave bridge in a Bruker SHQ0601 cavity equipped with an Oxford Instruments continuous flow cryostat and using an ITC 503 temperature controller (Oxford Instruments). Measurement temperatures ranged from 5 to 30 K, using liquid helium as coolant. The spectrometer was controlled by the Xep software package (Bruker).

Spin quantification – The spin concentration of the different samples was quantified by double integration of the EPR signal recorded at 100 μW at 10 K and comparison to the EPR signal of a Cu^{2+} standard (100 μM CuSO_4 , 2mM EDTA) recorded under identical conditions. The H_{ox} -like signal was isolated in the $[2\text{Fe}]^{\text{pdt}}$ -HydA1 and $[2\text{Fe}]^{\text{adt}}$ -HydA1 whole cell spectra by subtracting the spectrum of apo-HydA1 containing cells recorded under identical conditions (as represented in Figure 2 spectra b and c; and Figure 4 spectra c and d).

EPR simulations – We simulated the various H_{ox} species identified in the spectra displayed in figure 2 and 4, further detailed in figures S-23 and S-24. We used the pepper program, part of the easyspin toolbox (version 5.2.11) in the software Matlab (Mathworks, Inc).^[14] We corrected the experimental magnetic field of all spectra using the DPPH standard provided by Bruker ($g=2.0036$).

Upon simulation, we accounted for the anisotropic spectral broadening of each species with the HStrain function. H-strain describes line shape as unresolved hyperfine couplings, and was chosen as Q-band spectra do not show significant broadening of the EPR lines compared to X-band spectra, unlike expected when line shape is governed by g-strain.^[14] The H-strain parameter corresponds to the full width at half maximum of the gaussian lines along the three principal g-tensor axes.

All parameters (6 for each state, 2 for each magnetic axis) were manually adjusted using the in vitro spectrum of either $[2\text{Fe}]^{\text{adt}}\text{-HydA1}_{\text{pur}}$ or $[2\text{Fe}]^{\text{pdt}}\text{-HydA1}_{\text{pur}}$ as reference. Only the signal amplitude and, when needed, the relative proportions of H_{ox} vs $\text{H}_{\text{ox}}\text{-CO}$ were then modified to match the spectra acquired on the in vivo samples.

References

- [1] A. Adamska-Venkatesh, D. Krawietz, J. Siebel, K. Weber, T. Happe, E. Reijerse, W. Lubitz, *J Am Chem Soc* **2014**, *136*, 11339-11346.
- [2] N. Khanna, C. Esmieu, L. S. Mészáros, P. Lindblad, G. Berggren, *Energy Environ. Sci.* **2017**, *10*, 1563-1567.
- [3] D. W. Mulder, M. W. Ratzloff, E. M. Shepard, A. S. Byer, S. M. Noone, J. W. Peters, J. B. Broderick, P. W. King, *J Am Chem Soc* **2013**, *135*, 6921-6929.
- [4] A. Adamska, A. Silakov, C. Lambertz, O. Rudiger, T. Happe, E. Reijerse, W. Lubitz, *Angew Chem Int Ed* **2012**, *51*, 11458-11462; *Angew Chem* **2012**, *124*, 11624-11629
- [5] C. Kamp, A. Silakov, M. Winkler, E. J. Reijerse, W. Lubitz, T. Happe, *Biochim Biophys Acta* **2008**, *1777*, 410-416.
- [6] L. Loiseau, S. Ollagnier-de Choudens, D. Lascoux, E. Forest, M. Fontecave, F. Barras, *J Biol Chem* **2005**, *280*, 26760-26769.
- [7] A. Le Cloirec, S. C. Davies, D. J. Evans, D. L. Hughes, C. J. Pickett, S. P. Best, S. Borg, *Chem. Commun.* **1999**, 2285-2286.
- [8] E. J. Lyon, I. P. Georgakaki, J. H. Reibenspies, M. Y. Darensbourg, *Angew Chem Int Ed* **1999**, *38*, 3178-3180; *Angew Chem* **1999**, *111*, 3373-3376
- [9] M. Schmidt, S. M. Contakes, T. B. Rauchfuss, *J. Am. Chem. Soc.* **1999**, *121*, 9736-9737.
- [10] H. Li, T. B. Rauchfuss, *J. Am. Chem. Soc.* **2002**, *124*, 726-727.
- [11] D. W. Mulder, D. O. Ortillo, D. J. Gardenghi, A. V. Naumov, S. S. Ruebush, R. K. Szilagy, B. Huynh, J. B. Broderick, J. W. Peters, *Biochemistry* **2009**, *48*, 6240-6248.
- [12] A. Hemschemeier, A. Melis, T. Happe, *Photosynth Res* **2009**, *102*, 523-540.
- [13] J. Esselborn, C. Lambertz, A. Adamska-Venkates, T. Simmons, G. Berggren, J. Noth, J. Siebel, A. Hemschemeier, V. Artero, E. Reijerse, M. Fontecave, W. Lubitz, T. Happe, *Nat Chem Biol* **2013**, *9*, 607-609.
- [14] S. Stoll, A. Schweiger, *J Magn. Res* **2006**, *178*, 42-55.